NIH Public Access
Author Manuscript
Circ Arrhythm Electrophysiol. Author manuscript; available in PMC 2015 December 01.

Published in final edited form as:
Circ Arrhythm Electrophysiol. 2014 December ; 7(6): 1205–1213. doi:10.1161/CIRCEP.113.001666.

Non-equilibrium reactivation of Na^+ current drives early afterdepolarizations in mouse ventricle

Andrew G. Edwards, PhD[1], **Eleonora Grandi, PhD**[3], **Johan E. Hake, PhD**[4], **Sonia Patel, BSc**[1], **Pan Li, PhD**[4], **Shigeki Miyamoto, PhD**[2], **Jeffrey H. Omens, PhD**[1], **Joan Heller Brown, PhD**[2], **Donald M. Bers, PhD**[3], and **Andrew D. McCulloch, PhD**[1]

[1]Department of Bioengineering, University of California, San Diego, USA [2]Department of Pharmacology, University of California, San Diego, USA [3]Department of Pharmacology, University of California, Davis, USA [4]Simula Research Laboratory, Center for Biomedical Computing, Lysaker, Norway [5]Department of Cardiology, University Medical Center Groningen, 9700 RB Groningen, The Netherlands

Abstract

Background—Early-afterdepolarizations (EADs) are triggers of cardiac arrhythmia driven by L-type Ca^{2+} current (I_{Ca_L}) reactivation or sarcoplasmic reticulum (SR) Ca^{2+} release and Na^+/Ca^{2+} exchange. In large mammals the positive action potential (AP) plateau promotes I_{Ca_L} reactivation, and the current paradigm holds that cardiac EAD dynamics are dominated by interaction between I_{Ca_L} and the repolarizing K^+ currents. However, EADs are also frequent in the rapidly repolarizing mouse AP, which should not readily permit I_{Ca_L} reactivation. This suggests that murine EADs exhibit unique dynamics, which are key for interpreting arrhythmia mechanisms in this ubiquitous model organism. We investigated these dynamics in myocytes from arrhythmia-susceptible CaMKIIδ_C-overexpressing mice (Tg), and via computational simulations.

Methods and Results—In Tg myocytes, β-adrenergic challenge slowed late repolarization, potentiated SR Ca^{2+} release, and initiated EADs below the I_{Ca_L} activation range (−47±0.7 mV). These EADs were abolished by caffeine and tetrodotoxin (but not Ranolazine), suggesting that SR Ca^{2+} release and Na^+ current (I_{Na}), but not late I_{Na}, are required for EAD initiation. Simulations suggest that potentiated SR Ca^{2+} release and Na^+/Ca^{2+} exchange triangulate late AP repolarization, which permits non-equilibrium reactivation of I_{Na}, and thereby drives the EAD upstroke. AP clamp experiments suggest that lidocaine eliminates virtually all inward current elicited by EADs, and that this effect occurs at concentrations (40-60 μM) for which lidocaine remains specific for inactivated Na^+ channels. This strongly suggests that previously inactive channels are recruited during the EAD upstroke, and that non-equilibrium I_{Na} dynamics underlie murine EADs.

Conclusions—Non-equilibrium reactivation of I_{Na} drives murine EADs.

Corresponding Author: Andrew G. Edwards, PhD, Department of Bioengineering, University of California, San Diego, 9500 Gilman Drive, La Jolla, CA 92093-0412, agedwards@ucsd.edu, phone: (858) 534-6616.

4.3 Disclosures

D.B received a research grant from Gilead Sciences in May 2013. Gilead Sciences was in no way involved in the design, funding, execution, or interpretation of this study.

NIH-PA Author Manuscript
NIH-PA Author Manuscript
NIH-PA Author Manuscript

NIH-PA Author Manuscript

NIH-PA Author Manuscript

NIH-PA Author Manuscript

Keywords

arrhythmia; cardiac dynamics; calcium; I_{Na}; EADs

Introduction

It is generally accepted that lethal ventricular arrhythmias occur when a triggering event is able to propagate into electrophysiologically susceptible tissue[1]. Premature ventricular contractions are prototypical triggers in the myocardium, and are thought to emerge from arrhythmogenic cellular events known as early and delayed afterdepolarizations (EADs or DADs)[2]. DADs occur in the diastolic interval and result from Na^+/Ca^{2+}exchange secondary to spontaneous sarcoplasmic reticulum Ca^{2+} release (SCR)[3]. In contrast, EADs initiate during action potential (AP) repolarization and involve complex dynamical interaction among the currents that remain available (or regain availability) late in the AP[4]. Humans and other large mammals exhibit ventricular APs with a prolonged plateau phase (~100-200 ms) at slightly positive membrane potentials (E_m). This imposes two key constraints on the inward currents capable of driving EADs in these species: (1) the fast sodium current (I_{Na}) is largely excluded as it remains entirely inactivated at plateau E_m[5]; (2) while Na^+/Ca^{2+}exchange can act as the proximal cause of EADs in large mammals[6, 7], peak inward Na^+/Ca^{2+}exchange current (I_{NaCa}) is thermodynamically limited because plateau E_m is relatively close to exchange equilibrium[3]. Thus, the L-type Ca^{2+} current (I_{Ca_L}) eventually carries the majority of inward charge during the EAD upstroke. As a consequence of these constraints, a series of recent studies has established that EADs in large mammals rely largely upon the dynamics governing reactivation of I_{Ca_L}[1,5,8].

In contrast, the murine ventricular AP repolarizes rapidly (tens of ms) and exhibits a brief plateau at negative E_m (~ −50 mV). These characteristics sharply limit the potential for I_{Ca_L} reactivation, yet numerous studies have observed EADs in the mouse[9-13], and most have implicated I_{Ca_L}[11-14]. This presents a paradox regarding the electrophysiologic conditions required to elicit EADs in the mouse ventricle, which has important implications for interpreting arrhythmia mechanisms in a large number of disease models. To clarify the dynamics capable of driving murine EADs, we have combined experimental and computational approaches to assess EAD mechanisms in myocytes from arrhythmia-susceptible CaMKIIδ_C-overexpressing mice (Tg)[15].

EADs appearing during β-adrenergic stimulation were initiated by non-equilibrium reactivation of I_{Na} secondary to exaggerated sarcoplasmic reticulum (SR) Ca^{2+} release and I_{NaCa}. In some instances this evoked subsequent reactivation of I_{Ca_L} and dynamical behavior similar to that described for larger species. However, the majority of events remained reliant upon non-equilibrium I_{Na} dynamics. Thus, we suggest that the mouse AP imposes unique constraints on EAD dynamics that rely upon an I_{Na}-dependent mechanism of initiation.

Methods

A detailed description of all methods and analyses are provided in the Supplemental Information (SI).

NIH-PA Author Manuscript

NIH-PA Author Manuscript

NIH-PA Author Manuscript

CaMKIIδ_C transgenic mice

Male and female cardiac-specific CaMKIIδ_C transgenic mice (n=135) and WT littermates (n=130) were studied at 60.4±0.6 days of age (both groups). These mice have previously been described in detail[15, 16], however, we note that they now exhibit a slower time course of HF development than originally published (Figure S4). All procedures received prior approval from the UCSD Animal Subjects Committee.

Myocyte Isolation, Electrophysiology, and Ca^{2+} imaging

CaMKIIδ_C myocytes were isolated via enzymatic dissociation, and stored for at least 2 hours at 37°C prior to undergoing one of two protocols: (1) Current clamp AP recordings in whole cell patch configuration, or (2) pause-induced spontaneous Ca^{2+} release under field-pacing (SCR). For patch clamp experiments, simultaneous Ca^{2+} imaging was performed via Fura-2 with internal solution containing (mmol/L) 120 K-Aspartate, 10 KCl, 10 NaCl, 5 Mg-ATP, 1 MgCl2, 0.3 Li-GTP, and 125 μM Fura-2 potassium salt (pH 7.2, KOH). The external solution for both patch-clamp and field-pacing experiments (Normal Tyrode's, NT) contained (*m*M) 140 NaCl, 4 KCl, 1 CaCl2, 1 MgCl2, 10 D-glucose, and 10 Hepes (pH: 7.4, NaOH). Isoproterenol (100 *n*M) was added from frozen stock (1 *m*M in 0.01N HCl), and caffeine (10 *m*M) was prepared fresh from powder. For both experiments cells were preloaded with Ca^{2+}-sensitive dyes in 37°C media: Fura-2 AM for patch-clamp (15 minutes, 5 μM, Life Technologies: F1225) and Fluo-3 AM for SCR (40 minutes, 5 μM, Life Technologies: F1241). Cells were then twice rinsed and stored in NT for 20 minutes to allow de-esterification. During current clamp experiments, cells were paced for 50 cycles (1 Hz) in NT before Iso was applied focally by micro-bore tubing. Another 50 cycles were acquired at least 1 minute after beginning Iso superfusion, as such all patch-clamp recordings are paired analyses. In SCR experiments, cells were paced for 30 seconds (again 1 Hz), and followed by a 30-second pause for SCR before rapid caffeine contracture (10 mM in 0 Na^+/0 Ca^{2+} Tyrode's). For SCR, Iso containing NT was applied to a separate group of cells from the same isolation. The bathing solution was maintained at 37°C for all experiments, and the experimenter was blinded to the genotype of the cells.

Computational Models

Our mouse ventricular cell model was a modification of the Bondarenko myocyte[17]. Alterations were made primarily to permit implementation of acute and chronic effects of CaMKII. These included phosphoregulation of the Ryanodine receptor (RyR), I_{CaL}, I_{Na}, and late I_{Na} (I_{NaL})[18-20], as well as transcriptional regulation of the transient outward current (I_{to}), inward rectifier current (I_{K1}), I_{NaCa}, and sarco-endoplasmic reticulum Ca^{2+}-ATPase (SERCA)[16, 20, 21]. β-adrenergic stimulation was simulated via established effects at I_{CaL}, the ultra-rapid delayed rectifier current (I_{Kur}), and on function of the Na^+/K^+-ATPase and SERCA. Importantly we did not implement any direct effects of βAR stimulation at I_{Na}. While previous work has suggested that βAR agonists induce both a leftward shift in voltage-dependent activation and inactivation, and increased peak conductance [22], these effects may be partially explained by CaMKII. In particular, CaMKII has recently been shown to be responsible for the Iso-dependent leftward shifted inactivation and increased I_{NaL} accompanying Iso challenge [22], and these actions are already incorporated in our I_{Na}

NIH-PA Author Manuscript

NIH-PA Author Manuscript

NIH-PA Author Manuscript

model. Additionally, the effects of β-adrenergic stimulation on peak conductance and activation have previously been shown to occur relatively slowly (appearing after ~ 5 minutes), and at least partly depend upon translocation of NaV1.5 to the cell surface [23, 24]. Because our experiments were generally complete 2-3 minutes after application of Iso, it is unlikely that these increases in channel density contributed to the EADs we've measured.

Statistics

Fisher's exact test was used for EAD susceptibility in terms of proportion of cells. The Kruskal-Wallis test was used for percent of cycles with EADs or DADs. This test was applied across all 4 groups (WT, Tg, WT + Iso, Tg + Iso), and followed by either Mann-Whitney (unpaired data) or Wilcoxon (paired data) post hoc tests, with Bonferroni correction. Due to larger sample sizes for SCR experiments, differences in incidence of SCR were determined by Chi-squared tests, and mean event frequencies (events/cell) were assessed by the Mann-Whitney test. Repeated measures ANOVA was used for action potential and Ca^{2+}-handling comparisons after separating the transgenic cells into EAD+ and EAD− subsamples (see Results). Student's t-tests were applied with Bonferroni correction for all *post hoc* comparisons.

Results

Cellular arrhythmogenesis in CaMKIIδC transgenic myocytes

The cardiac-specific CaMKIIδ_C transgenic mouse develops heart failure (HF), is arrhythmia-susceptible, and presents increased cellular susceptibility to both EADs and DADs[10, 16, 20, 21] (Figure S4). Here we elicited EADs through β-adrenergic challenge by isoproterenol (100 nM, Iso; Figure 1A & B), and while DADs and SCR were almost completely absent in patch-clamp experiments (19 events in 1881 cycles, Tg vs. WT: p = 0.34), Tg myocytes were more susceptible to pause-induced SCR during Iso treatment (Figure 1C). Importantly, the ability of Iso to induce both arrhythmogenic behaviors was associated with normalization of a baseline deficit in SR Ca^{2+} content in Tg cells (Figure 1C, bottom right). This suggests that an Iso-induced increase in SR Ca^{2+} load may be central to both forms of electrophysiologic instability.

Enhanced Ca^{2+} handling and prolonged repolarization precede EAD initation

To describe the changes in steady-state Ca^{2+} handling and AP morphology associated with EADs, we separated the Tg cells into those that did exhibit EADs (EAD+, n=12), and did not exhibit EADs (EAD−, n=15) in at least 10% of cycles. These two Tg cell populations were compared with all WT cells (n=17). In EAD+ recordings, steady-state data were taken from the 5-10 cycles immediately prior to the first EAD, for all other cells we used the final 5-10 cycles of the recording. These analyses suggest that murine EAD susceptibility is associated with exaggerated Ca^{2+} cycling and slowed late repolarization immediately before EAD initiation (Figure 2). At baseline (normal Tyrode's), Ca^{2+} transients were smaller and slower to decay in EAD+ cells compared with WT. The baseline AP in EAD+ cells also exhibited slower early repolarization, although late repolarization was not different from WT (p = 0.13). As expected, Iso increased Ca^{2+} transient amplitude and accelerated Ca^{2+} decay in WT cells. These effects were exaggerated in EAD+ cells such that, immediately

NIH-PA Author Manuscript

NIH-PA Author Manuscript

NIH-PA Author Manuscript

before initiation of EADs, Iso had normalized the baseline deficits in both Ca^{2+} transient amplitude and decay rate. This resulted in an Iso-induced increase in transient amplitude that was more than doubled in EAD+ cells relative to WT (Figure 2A, bottom right, and Figure 2B, top right). AP prolongation accompanied these Iso-dependent Ca^{2+} handling changes in both WT and Tg cells, and again this effect was amplified in EAD+ cells, particularly for late repolarization where APD_{90} was 53% longer than in Iso-treated WT myocytes ($p < 0.05$).

SR Ca^{2+} release is required for murine EADs

These steady-state effects suggest that Iso elicits EADs in Tg cells by enhancing Ca^{2+} cycling in a manner that destabilizes repolarization. However, all observed Ca^{2+} handling and AP changes could be due to gain-of-function regulation at either I_{CaL} or SR Ca^{2+} release, both of which are recognized consequences of CaMKII activation[16, 25, 26], and are the primary drivers of EADs in large mammals[6, 7, 27].

The low late AP plateau in Iso (Figure 2B, top) is probably due to greater SR Ca^{2+} release and prolonged inward I_{NaCa}, as suggested by earlier investigations[28, 29]. To test whether this plays a role in driving the observed EADs, we rapidly applied caffeine to a cell exhibiting Iso-induced EADs. This maneuver simultaneously eliminates inward currents driven by SR Ca^{2+} release, and potentiates I_{CaL} by reducing Ca^{2+}-dependent inactivation - thus exaggerating any I_{CaL}-dependent EAD mechanism. Figure 3 shows that caffeine caused the expected large Ca^{2+} release, and thereby triggered an AP. The sustained elevation of $[Ca^{2+}]_i$ during the contracture greatly prolonged repolarization (Figure 3A). However, while caffeine lingered after the return to pacing (preventing SR Ca^{2+} reloading) EADs were abolished. Thus, SR Ca^{2+} release is essential for EAD initiation, but potentiated I_{CaL} is not sufficient to generate EADs in the absence of SR Ca^{2+} release.

The changes in AP morphology resulting from caffeine also support the contention that SR Ca^{2+} release promotes EADs by altering the trajectory of late repolarization. Figure 3C shows that caffeine elicits inverse effects upon early and late repolarization. APD_{50} is dramatically increased, presumably due to less Ca^{2+}-dependent inactivation of I_{CaL}, whereas the I_{NaCa}-driven late plateau is removed (with repolarization parallel to the baseline AP trajectory). Thus, Iso causes larger SR Ca^{2+} release and inward I_{NaCa}, which suspends terminal repolarization.

Unique dynamics of murine EADs

The observed EADs could be discriminated by whether or not they exhibited sustained Ca^{2+} transients, and we reasoned that this may indicate two populations of EADs caused by distinct mechanisms. Of the 198 EAD-containing cycles, 20.7% exhibited a sustained Ca^{2+} transient - type 1 EAD morphology (Figure 4A, left). The remaining EADs (79.3%) exhibited normal monotonic Ca^{2+} transient decay, and shorter E_m plateaus with fewer oscillations (Figure 4A, right) - type 2 EADs. Importantly, the take-off (TO) potentials of the first oscillations in both types were below the I_{CaL} activation range, at −46.4 and −47.7 mV for types 1 and 2, respectively (Figure 4B, right). This further indicates that I_{CaL} reactivation is unlikely to contribute to EAD initiation in either type of event. For type 1

NIH-PA Author Manuscript

NIH-PA Author Manuscript

NIH-PA Author Manuscript

EADs, subsequent oscillations took off from more positive potentials, whereas they became progressively more negative in type 2 EADs. Together, these observations indicate two characteristics of murine EADs that distinguish them from EADs in large mammals: (1) the initiating event relies upon dynamics that cannot be explained by I_{Ca_L} reactivation, and (2) while I_{Ca_L} reactivation may contribute to EAD maintenance in cycles with sustained Ca^{2+} transients (type 1), a separate dynamical mechanism can support multiple oscillations in type 2 EADs.

Temporal changes in oscillation amplitude and period provide further support for the existence of multiple dynamical mechanisms in the mouse. A signature of I_{Ca_L}-dependent EAD dynamics in large mammals is that, within a given AP, EAD oscillations increase in both amplitude and period before spontaneously terminating. These properties have been described in terms of non-linear dynamics, which suggest that the I_{Ca_L} and K^+ current interactions evolve through a destabilizing Hopf bifurcation, from which oscillation amplitude and period increase before terminating at a homoclinic bifurcation[5]. Figure 4C (left) shows that, while both types of EAD exhibit similarly large initiating oscillations, only type 1 EADs also present the characteristic increase in amplitude from the mid-point oscillation to the final oscillation of the cycle. Oscillation period increases from the first oscillation to the last in both types of EAD, although the first oscillation is more rapid in the type 2 events compared to type 1 (Figure 4C, right). In sum, these analyses suggest that the two types of EAD are initiated by a common dynamical mechanism that does not require I_{Ca_L}, but that type 1 EADs then recruit I_{Ca_L} and exhibit late dynamics that are very similar to those observed in larger mammals.

SR Ca^{2+} release slows late repolarization and recruits I_{Na} to initiate EADs

Because the mechanism of EAD initiation requires SR Ca^{2+} release, and occurs at negative potentials which favor forward-mode Na^+/Ca^{2+}exchange, I_{NaCa} is an obvious candidate for driving EAD initiation. However, it is unlikely that the conventionally small, slow, and monotonically decaying forward mode I_{NaCa} could elicit the large and fast depolarizations observed here. Thus, it is more likely that Ca^{2+} release and I_{NaCa} contribute by "conditioning" late repolarization to permit reactivation of another major inward current[6]. To interrogate these dynamics quantitatively, we developed a computational model of the mouse ventricular myocyte (see Methods and SI for details of this implementation).

The EADs produced by this model recapitulated the more frequent type 2 EAD morphology. Figure 5A shows the transition to EAD behavior (at beat 13 of 50), as Ca^{2+} transient amplitude increases during simulated Iso. These EADs exhibit variable morphology but initiate at potentials between −40 and −45 mV, and occur 30 to 50 ms after the current injection used to trigger the AP (Figure 5B, 2 vs. 3). Further, they appear quasi-stochastically for the first several beats after transition, which is a signature of the chaotic determinism that is proposed to be a general characteristic of EAD dynamics[8]. Acutely removing the CaMKII-specific effects on I_{Ca_L} was not sufficient to abolish EADs in the model (6 vs. 3), whereas computational ablation of either SR Ca^{2+} release (4 vs. 3), or I_{NaCa} (5 vs. 3) did eliminate EADs. Notably, I_{NaCa} elicits both AP prolongation and EAD initiation via recruitment of I_{Na}, which exhibits a progressive induction and then clear

NIH-PA Author Manuscript

NIH-PA Author Manuscript

NIH-PA Author Manuscript

bifurcation (Figure 5C) as Ca^{2+} transient amplitude, SR Ca^{2+} release, and I_{NaCa} increase. While I_{NaCa} is well known to mediate Ca^{2+}-dependent modulation of late AP duration in the mouse[9, 30-32], this interaction between I_{NaCa} and I_{Na} reactivation is not widely appreciated as contributor to AP prolongation in the mouse. However, these simulations suggest that, even prior to EAD initiation, inward current contributed by reactivating I_{Na} is responsible for much more of the observed AP prolongation than I_{NaCa} (Figure 5C, first and second columns). I_{CaL} was also reactivated to a small extent during EADs, but this is secondary to I_{Na}. We were unable to find an EAD regime that replicated the less frequent type 1 EAD morphology, and we suggest that this behavior may require a more complex representation of EC coupling than is present in this model, which does not permit prolonged or reactivating SR Ca^{2+} release (see SI 2.1.2).

EAD initiation is carried by non-equilibrium reactivation of I_{Na}

To experimentally test the model prediction that I_{Na} is responsible for driving EAD initiation, we attempted to interrupt Iso-induced EADs by applying I_{Na} inhibitors of differing selectivity for the late and fast components of I_{Na}. In the same cell we first rapidly applied 10 *μM* Ranolazine, and after brief washout, introduced tetrodotoxin (TTX) at 100 nM, 1 *μM*, and 5 *μM* (Figure 6). Ranolazine exhibits greater selectivity for I_{NaL}[33], and at 1 Hz, 10 *μM* Ranolazine achieves approximately 70% attenuation of I_{NaL} but near negligible inhibition of peak I_{Na}[34]. Figure 6A shows that, while this treatment clearly inhibited prolonged EADs, it did not prevent EAD initiation (trace 2 vs. 1). Similarly, TTX at a dose capable of inhibiting neuronal I_{Na} (100 nM[35]) did not prevent the EAD upstroke (Figure 6A, trace 3). However, TTX eliminated

EADs at a dose (1 *μM*) approximately sufficient for half inhibition of peak myocardial I_{Na} and 30% inhibition of I_{NaL}[36] (Figure 6A, traces 4 and 5 - full recordings are provided in Figure S5). The ability of TTX to eliminate EADs was reproducible - 3/3 cells were returned to normal AP morphology upon rapid application of TTX (Figure S6). Thus, while I_{NaL} may contribute to the dynamics of plateau EADs by contributing inward current late in the AP, this component of the Na^+ current is not responsible for initiating murine EADs. Instead it appears that EAD initiation is carried by reactivation of canonical fast I_{Na}.

While these reactivations initiate above the E_m range that typically permits steady-state I_{Na} availability, non-equilibrium reactivation of myocardial I_{Na} is known to occur in both normal and pathologically mutated $Na_{V1.5}$ channels[37]. Returning to our model, we confirmed that an acute 50% reduction in I_{Na} conductance eliminated EADs as in the experiments (Figure 6B(b)), and observed that the state occupancies of the I_{Na} model support the contention that non-equilibrium I_{Na} reactivation is responsible for EAD initiation. Figure 6B(c) shows that the fast open state (O) repopulates prior to the burst-mode open state (LO), and achieves ~5 times greater peak state occupancy during the EAD upstroke. These channel reopenings are fueled by slight recovery through the canonical closed states (C1-C3, Figure S7).

To test this model result experimentally we performed AP clamp experiments with one of the recorded EAD waveforms in the presence of various concentrations of lidocaine. This I_{Na} antagonist is largely selective for inactivated channels[38, 39] and as shown in Figure 6C(a)

NIH-PA Author Manuscript

NIH-PA Author Manuscript

NIH-PA Author Manuscript

it is clear that the EAD upstroke in these AP clamps induces a significant lidocaine-sensitive inward current, even below the concentration range that inhibits non-inactivated channels[39]. Further, applying the same experimental AP waveform to clamp the I_{Na} model achieves similar reactivation characteristics (Figure 6C(b)). Importantly, these reactivation dynamics were not attributable to the modeled effects of CaMKII at the Na^+ channel. Rather the established leftward-shifts in steady-state activation and inactivation[21], and slower recovery from inactivation, both of which are incorporated into the Tg I_{Na} model, serve to limit non-equilibrium reactivation. Figure 7A shows that reactivation is exaggerated in the isolated WT I_{Na} model compared to the Tg model during AP clamp of the first Tg EAD waveform. As described previously, the propensity for this reactivation is highly dependent on the trajectory of repolarization[37].

To investigate whether differences between the mouse and large mammal APs should be expected to alter the impact of CaMKII on these reactivation dynamics, we applied repolarizing voltage ramps of differing trajectories to the I_{Na} models[37]. As shown in Figure 7B, a slowly repolarizing ramp (− 1 V/s) after prolonged depolarization (panel a) elicited much less non-equilibrium reactivation than more rapid (~ −2 or −4 V/s) repolarizations with no preceding plateau (panel b). In both protocols the Tg model exhibited reduced reactivation of the canonical open state (O), but because these reactivations were much smaller for both Tg and WT in the slower ramp, the enhanced late current (LO) in the Tg model caused the overall I_{Na} to be much larger for Tg in the slower, pseudo-large mammal waveform. Finally, when the WT I_{Na} model is substituted into the current-clamped Tg cell model, the exaggerated reactivation described in Figure 7 further disrupts normal repolarization (Figure S8).

Discussion

Here we have used an established arrhythmogenic mouse model and computational simulations to describe the unique constraints that murine electrophysiology imposes on mechanisms of EAD generation. We found that, unlike EADs in large mammals, the rapidly repolarizing murine AP dramatically reduces the potential for I_{Ca_L} reactivation to drive EADs. Instead EADs are initiated by non-equilibrium reactivation of I_{Na} in the mouse ventricle, and this depends critically on the ability of SR Ca^{2+} release to modulate the trajectory of late repolarization. These findings provide a key framework for interpreting mechanisms of arrhythmogenesis in existing and future mouse models of disease.

The role of SR Ca^{2+} release in EAD dynamics has been appreciated for more than 20 years[40, 41]. In large mammals, triggered Ca^{2+} release is thought to promote EADs in one of two ways: (1) potentiated, but still synchronous, Ca^{2+} release and inward I_{NaCa} can be sufficient to disrupt the balance of currents during the AP plateau, and thereby "condition" repolarization to enter the dynamical regime involving I_{Ca_L} (see Volders et al., for review[6]), or (2) Ca^{2+} release becomes spatiotemporally disco-ordinated, such that Ca^{2+} waves occur during AP repolarization, which again drives I_{NaCa} and may recruit accessory inward currents[7]. While we have not assessed the potential for Ca^{2+} waves to contribute to the EADs observed here, the time-scale upon which these events develop suggest that they are unlikely to have contributed to EAD initiation. The first EAD oscillation typically occurred

NIH-PA Author Manuscript

NIH-PA Author Manuscript

NIH-PA Author Manuscript

between 30 and 50 ms after the triggering current pulse in our experiments, whereas spontaneous Ca^{2+} waves exhibit slower kinetics in which peak $[Ca^{2+}]_i$ develops over hundreds of milliseconds.

Thus, any spontaneous event not detected before the AP was stimulated would quickly be overwhelmed by the Ca^{2+} release triggered by excitation. It is possible that wavelike dynamics contribute to plateau oscillations in type 1 EADs, but these events still require initiation by the faster dynamical mechanism. Thus, we contend that the suspended repolarization due to sustained I_{NaCa} is more likely to describe how SR Ca^{2+} release contributes to EAD dynamics in the mouse. This mechanism also explains how gain-of-function changes to I_{CaL} gating and/or expression can promote murine EADs without eliciting I_{CaL} reactivation. That is, by potentiating SR Ca^{2+} release through increased SR Ca^{2+} load and fractional release. It is for this reason, and the well known promiscuity of available Ca^{2+} channel antagonists[42, 43] that we have avoided experiments involving I_{CaL} antagonists in this study. As such, we strongly recommend against interpreting the ability of I_{CaL} inhibitors to reduce EAD incidence in the mouse as inferring a role for I_{CaL} reactivation in driving murine EADs.

While cardiac EADs have most commonly been associated with the late component of I_{Na}[33], previous studies have also recognized that reactivation of fast I_{Na} may be involved in certain contexts. Most clearly, the LQT3 mutation I1768V exhibits exaggerated non-equilibrium reactivation during slow ramp repolarization, but appears innocuous by standard square-pulse characterization. Simulation of these properties within the Luo-Rudy guinea pig ionic model recapitulated AP prolongation at normal sinus rates and yielded EADs in simulated bradycardia[37]. More generally, early studies suggested that reactivation of I_{Na} may drive EADs initiating at more negative potentials in large mammals[6, 40]. However, these mechanisms were quickly thought to be less physiologically important because they required more severe conditions to be induced[40] - as might be expected of any mechanism that depends on I_{Na} recovery after the prolonged AP plateau. Together, these prior studies suggest that, in large mammals, the conditions required to achieve non-equilibrium reactivation of I_{Na} are probably supra-physiologic in all but a few disease contexts. In contrast, the triangular mouse AP both accelerates recovery of I_{Na} and reduces the potential for I_{CaL} reactivation, hence shifting EAD dynamics to favor reactivation of I_{Na}. As a result, we conclude that, for any conditioning stimulus (exaggerated SR Ca^{2+} release and I_{NaCa} in the CaMKIIδ_C transgenic model used here), non-equilibrium I_{Na} dynamics are the most likely basis for EAD initiation in the mouse. Furthermore, our simulations suggest that these I_{Na} dynamics are responsible for the majority of late AP prolongation in the mouse under conditions of exaggerated Ca^{2+} cycling, particularly β-adrenergic challenge. This finding may be important for many murine simulation studies, where I_{Na} models that are not capable of representing non-equilibrium reactivation are unlikely to capture Ca^{2+}-induced AP prolongation within reasonable constraint of I_{NaCa} and other currents that are active late in the AP.

A key question for the general importance of these findings is whether non-equilibrium reactivation is facilitated by CaMKII, and thus, whether this behavior may be specific to this Tg mouse model. To date, no data are available to describe a role for CaMKII in non-

NIH-PA Author Manuscript

NIH-PA Author Manuscript

NIH-PA Author Manuscript

equilibrium reactivation, and we have not assessed it experimentally in this study. However, the loss-of-function effects that CaMKII exerts on steady state I_{Na} would be expected to impair rather than facilitate non-equilibrium reactivation[21], and our simulations in the WT and Tg I_{Na} models support this assertion (Figure 7). Thus, while investigation of the potential for CaMKII to alter non-equilibrium gating of I_{Na} is warranted, there is currently little reason to expect such an outcome. Rather we believe these I_{Na} dynamics are a general property of murine electrophysiology, which depends on the trajectory of AP repolarization rather than CaMKII-dependent alteration of I_{Na} gating properties.

Supplementary Material

Refer to Web version on PubMed Central for supplementary material.

4.1 Acknowledgements

We thank Kevin P. Vincent for his careful auditing of our computational model.

4.2 Sources of Funding

This work was supported by a National Institutes of Health (5P01HL46345-12, A.M; P01-HL080101, J.H.B and D.B; R01-HL105242, A.M and D.B), the Fondation Leducq Translatlantic CaMKII Alliance (D.B), and postdoctoral fellowships from the American Heart Association and Heart Rhythm Society (A.E).

References

1. Sato D, Xie LH, Nguyen TP, Weiss JN, Qu Z. Irregularly appearing early afterdepolarizations in cardiac myocytes: Random fluctuations or dynamical chaos? Biophysical journal. 2010; 99:765–773. [PubMed: 20682253]
2. Nattel S, Maguy A, Le Bouter S, Yeh YH. Arrhythmogenic ion-channel remodeling in the heart: Heart failure, myocardial infarction, and atrial fibrillation. Physiological reviews. 2007; 87:425–456. [PubMed: 17429037]
3. Bers DM. Calcium cycling and signaling in cardiac myocytes. Annual review of physiology. 2008; 70:23–49.
4. Weiss JN, Garfinkel A, Karagueuzian HS, Chen PS, Qu Z. Early afterdepolarizations and cardiac arrhythmias. Heart rhythm : the official journal of the Heart Rhythm Society. 2010; 7:1891–1899. [PubMed: 20868774]
5. Tran DX, Sato D, Yochelis A, Weiss JN, Garfinkel A, Qu Z. Bifurcation and chaos in a model of cardiac early afterdepolarizations. Physical review letters. 2009; 102:258103. [PubMed: 19659123]
6. Volders PG, Vos MA, Szabo B, Sipido KR, de Groot SH, Gorgels AP, Wellens HJ, Lazzara R. Progress in the understanding of cardiac early afterdepolarizations and torsades de pointes: Time to revise current concepts. Cardiovascular research. 2000; 46:376–392. [PubMed: 10912449]
7. Zhao Z, Wen H, Fefelova N, Allen C, Baba A, Matsuda T, Xie LH. Revisiting the ionic mechanisms of early afterdepolarizations in cardiomyocytes: Predominant by ca waves or ca currents? American journal of physiology. Heart and circulatory physiology. 2012; 302:H1636–1644. [PubMed: 22307670]
8. Sato D, Xie LH, Sovari AA, Tran DX, Morita N, Xie F, Karagueuzian H, Garfinkel A, Weiss JN, Qu Z. Synchronization of chaotic early afterdepolarizations in the genesis of cardiac arrhythmias. Proceedings of the National Academy of Sciences of the United States of America. 2009; 106:2983–2988. [PubMed: 19218447]
9. Pott C, Muszynski A, Ruhe M, Bogeholz N, Schulte JS, Milberg P, Monnig G, Fabritz L, Goldhaber JI, Breithardt G, Schmitz W, Philipson KD, Eckardt L, Kirchhof P, Muller FU. Proarrhythmia in a non-failing murine model of cardiac-specific na+/ca 2+ exchanger overexpression: Whole heart and cellular mechanisms. Basic research in cardiology. 2012; 107:247. [PubMed: 22327339]

NIH-PA Author Manuscript

NIH-PA Author Manuscript

NIH-PA Author Manuscript

10. Sag CM, Wadsack DP, Khabbazzadeh S, Abesser M, Grefe C, Neumann K, Opiela MK, Backs J, Olson EN, Brown JH, Neef S, Maier SK, Maier LS. Calcium/calmodulin-dependent protein kinase ii contributes to cardiac arrhythmogenesis in heart failure. Circulation. Heart failure. 2009; 2:664–675. [PubMed: 19919992]
11. Said M, Becerra R, Valverde CA, Kaetzel MA, Dedman JR, Mundina-Weilenmann C, Wehrens XH, Vittone L, Mattiazzi A. Calcium-calmodulin dependent protein kinase ii (camkii): A main signal responsible for early reperfusion arrhythmias. Journal of molecular and cellular cardiology. 2011; 51:936–944. [PubMed: 21888910]
12. Thomas G, Gurung IS, Killeen MJ, Hakim P, Goddard CA, Mahaut-Smith MP, Colledge WH, Grace AA, Huang CL. Effects of l-type ca2+ channel antagonism on ventricular arrhythmogenesis in murine hearts containing a modification in the scn5a gene modelling human long qt syndrome 3. The Journal of physiology. 2007; 578:85–97. [PubMed: 17110414]
13. Wu Y, Temple J, Zhang R, Dzhura I, Zhang W, Trimble R, Roden DM, Passier R, Olson EN, Colbran RJ, Anderson ME. Calmodulin kinase ii and arrhythmias in a mouse model of cardiac hypertrophy. Circulation. 2002; 106:1288–1293. [PubMed: 12208807]
14. Killeen MJ, Gurung IS, Thomas G, Stokoe KS, Grace AA, Huang CL. Separation of early afterdepolarizations from arrhythmogenic substrate in the isolated perfused hypokalaemic murine heart through modifiers of calcium homeostasis. Acta physiologica. 2007; 191:43–58. [PubMed: 17524066]
15. Zhang T, Maier LS, Dalton ND, Miyamoto S, Ross J Jr. Bers DM, Brown JH. The deltac isoform of camkii is activated in cardiac hypertrophy and induces dilated cardiomyopathy and heart failure. Circulation research. 2003; 92:912–919. [PubMed: 12676814]
16. Maier LS, Zhang T, Chen L, DeSantiago J, Brown JH, Bers DM. Transgenic camkiideltac overexpression uniquely alters cardiac myocyte ca2+ handling: Reduced sr ca2+ load and activated sr ca2+ release. Circulation research. 2003; 92:904–911. [PubMed: 12676813]
17. Bondarenko VE, Rasmusson RL. Transmural heterogeneity of repolarization and ca2+ handling in a model of mouse ventricular tissue. American journal of physiology. Heart and circulatory physiology. 2010; 299:H454–469. [PubMed: 20525874]
18. Grandi E, Puglisi JL, Wagner S, Maier LS, Severi S, Bers DM. Simulation of ca-calmodulin-dependent protein kinase ii on rabbit ventricular myocyte ion currents and action potentials. Biophysical journal. 2007; 93:3835–3847. [PubMed: 17704163]
19. Koval OM, Snyder JS, Wolf RM, Pavlovicz RE, Glynn P, Curran J, Leymaster ND, Dun W, Wright PJ, Cardona N, Qian L, Mitchell CC, Boyden PA, Binkley PF, Li C, Anderson ME, Mohler PJ, Hund TJ. Ca2+/calmodulin-dependent protein kinase ii-based regulation of voltage-gated na+ channel in cardiac disease. Circulation. 2012; 126:2084–2094. [PubMed: 23008441]
20. Wagner S, Hacker E, Grandi E, Weber SL, Dybkova N, Sossalla S, Sowa T, Fabritz L, Kirchhof P, Bers DM, Maier LS. Ca/calmodulin kinase ii differentially modulates potassium currents. Circulation. Arrhythmia and electrophysiology. 2009; 2:285–294. [PubMed: 19808479]
21. Wagner S, Dybkova N, Rasenack EC, Jacobshagen C, Fabritz L, Kirchhof P, Maier SK, Zhang T, Hasenfuss G, Brown JH, Bers DM, Maier LS. Ca2+/calmodulin-dependent protein kinase ii regulates cardiac na+ channels. The Journal of clinical investigation. 2006; 116:3127–3138. [PubMed: 17124532]
22. Dybkova N, Wagner S, Backs J, Hund TJ, Mohler PJ, Sowa T, Nikolaev VO, Maier LS. Tubulin polymerization disrupts cardiac beta-adrenergic regulation of late ina. Cardiovascular research. 2014
23. Baba S, Dun W, Boyden PA. Can pka activators rescue na+ channel function in epicardial border zone cells that survive in the infarcted canine heart? Cardiovascular research. 2004; 64:260–267. [PubMed: 15485685]
24. Zhou J, Yi J, Hu N, George AL Jr. Murray KT. Activation of protein kinase a modulates trafficking of the human cardiac sodium channel in xenopus oocytes. Circulation research. 2000; 87:33–38. [PubMed: 10884369]
25. Dzhura I, Wu Y, Colbran RJ, Balser JR, Anderson ME. Calmodulin kinase determines calcium-dependent facilitation of l-type calcium channels. Nature cell biology. 2000; 2:173–177.

NIH-PA Author Manuscript NIH-PA Author Manuscript NIH-PA Author Manuscript

26. van Oort RJ, McCauley MD, Dixit SS, Pereira L, Yang Y, Respress JL, Wang Q, De Almeida AC, Skapura DG, Anderson ME, Bers DM, Wehrens XH. Ryanodine receptor phosphorylation by calcium/calmodulin-dependent protein kinase ii promotes life-threatening ventricular arrhythmias in mice with heart failure. Circulation. 2010; 122:2669–2679. [PubMed: 21098440]
27. Xie LH, Chen F, Karagueuzian HS, Weiss JN. Oxidative-stress-induced afterdepolarizations and calmodulin kinase ii signaling. Circulation research. 2009; 104:79–86. [PubMed: 19038865]
28. Noble D. Influence of na/ca exchange stoichiometry on model cardiac action potentials. Annals of the New York Academy of Sciences. 2002; 976:133–136. [PubMed: 12502551]
29. Schouten VJ, ter Keurs HE. The slow repolarization phase of the action potential in rat heart. The Journal of physiology. 1985; 360:13–25. [PubMed: 3989712]
30. Ferreiro M, Petrosky AD, Escobar AL. Intracellular ca2+ release underlies the development of phase 2 in mouse ventricular action potentials. American journal of physiology. Heart and circulatory physiology. 2012; 302:H1160–1172. [PubMed: 22198177]
31. Pott C, Ren X, Tran DX, Yang MJ, Henderson S, Jordan MC, Roos KP, Garfinkel A, Philipson KD, Goldhaber JI. Mechanism of shortened action potential duration in na+-ca2+ exchanger knockout mice. American journal of physiology. Cell physiology. 2007; 292:C968–973. [PubMed: 16943244]
32. Yao A, Su Z, Nonaka A, Zubair I, Lu L, Philipson KD, Bridge JH, Barry WH. Effects of overexpression of the na+-ca2+ exchanger on [ca2+]i transients in murine ventricular myocytes. Circulation research. 1998; 82:657–665. [PubMed: 9546374]
33. Zaza A, Belardinelli L, Shryock JC. Pathophysiology and pharmacology of the cardiac "late sodium current. Pharmacology & therapeutics. 2008; 119:326–339. [PubMed: 18662720]
34. Antzelevitch C, Belardinelli L, Zygmunt AC, Burashnikov A, Di Diego JM, Fish JM, Cordeiro JM, Thomas G. Electrophysiological effects of ranolazine, a novel antianginal agent with antiarrhythmic properties. Circulation. 2004; 110:904–910. [PubMed: 15302796]
35. Brette F, Orchard CH. No apparent requirement for neuronal sodium channels in excitation-contraction coupling in rat ventricular myocytes. Circulation research. 2006; 98:667–674. [PubMed: 16484618]
36. Wu L, Ma J, Li H, Wang C, Grandi E, Zhang P, Luo A, Bers DM, Shryock JC, Belardinelli L. Late sodium current contributes to the reverse rate-dependent effect of ikr inhibition on ventricular repolarization. Circulation. 2011; 123:1713–1720. [PubMed: 21482963]
37. Clancy CE, Tateyama M, Liu H, Wehrens XH, Kass RS. Non-equilibrium gating in cardiac na+ channels: An original mechanism of arrhythmia. Circulation. 2003; 107:2233–2237. [PubMed: 12695286]
38. Bean BP, Cohen CJ, Tsien RW. Lidocaine block of cardiac sodium channels. The Journal of general physiology. 1983; 81:613–642. [PubMed: 6306139]
39. Moreno JD, Zhu ZI, Yang PC, Bankston JR, Jeng MT, Kang C, Wang L, Bayer JD, Christini DJ, Trayanova NA, Ripplinger CM, Kass RS, Clancy CE. A computational model to predict the effects of class i anti-arrhythmic drugs on ventricular rhythms. Science translational medicine. 2011; 3:98ra83.
40. January CT, Chau V, Makielski JC. Triggered activity in the heart: Cellular mechanisms of early after-depolarizations. European heart journal. 1991; 12(Suppl F):4–9. [PubMed: 1725155]
41. Priori SG, Corr PB. Mechanisms underlying early and delayed afterdepolarizations induced by catecholamines. The American journal of physiology. 1990; 258:H1796–1805. [PubMed: 2163219]
42. Hata T, Makino N, Nakanishi H, Yanaga T. Modulation of na+-ca2+ exchange in cardiac sarcolemmal vesicles by ca2+ antagonists. Molecular and cellular biochemistry. 1988; 84:65–76. [PubMed: 2852769]
43. Rusck M, Juhsz O, Orlick J, Zachar J. Inhibition of na+-ca2+ exhcange by calcium antagonists in rat brain microsomal membranes. General Physiology Biophysics. 1986; 5:529–535. [PubMed: 2433186]

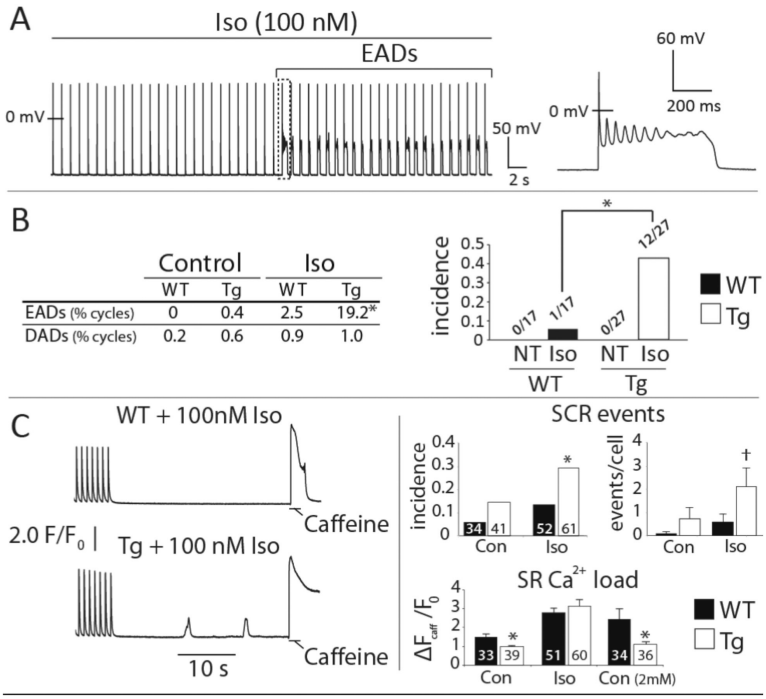

Figure 1.

CaMKIIδ_C myocytes are susceptible to EADs and SCR. A. Representative Tg cell transitioning to EADs during Iso challenge. B. EAD frequency (% of all cycles, left) and incidence (right) was increased in Tg compared to WT cells during Iso. Neither group exhibited EADs in Normal Tyrode's (NT). C. Left: representative Ca^{2+} recordings during pause-induced SR Ca^{2+} release experiments. Right: summary data for SCR incidence (fraction of cells with 1 or more SCR events), SCR frequency (events/cell), and SR Ca^{2+} content at baseline, during Iso, and in elevated extracellular Ca^{2+} (2 mM, SR Ca^{2+} content only). Cell numbers are inset to each bar. $^{**}p < 0.01$, $^{*}p < 0.05$, † $p = 0.06$. Data are mean ±SEM.

NIH-PA Author Manuscript NIH-PA Author Manuscript NIH-PA Author Manuscript

NIH-PA Author Manuscript
NIH-PA Author Manuscript
NIH-PA Author Manuscript

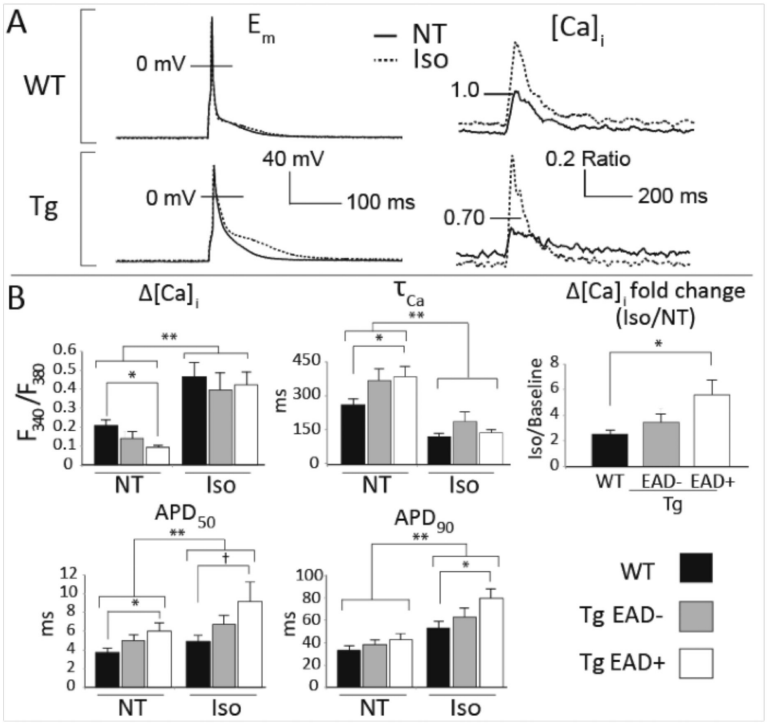

Figure 2.

EAD susceptibility is associated with exaggerated Ca^{2+} cycling and slowed late repolarization. A. Representative steady-state APs and Ca^{2+}transients. The smaller and more slowly decaying baseline Ca^{2+} transients in EAD+ cells are normalized by Iso, and associated with suspended late repolarization. B. Summary data for steady-state APs and Ca^{2+}handling. † pairwise contrast $p = 0.05$, * pairwise contrast $p < 0.05$, ** main effect of Iso $p < 0.05$. Data are mean±SEM.

NIH-PA Author Manuscript

NIH-PA Author Manuscript

NIH-PA Author Manuscript

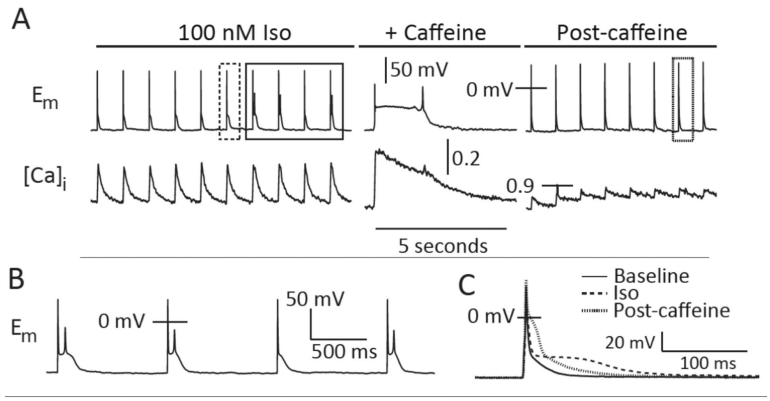

Figure 3.

SR Ca^{2+} release is required for EAD initiation. A. Caffeine (10 mM) eliminates EADs by depleting the SR Ca^{2+} store. B. EADs from the solid boxed region in panel A. C. AP morphologies from the NT (solid line), Iso (dashed line), and post-caffeine (dotted line) records. Iso and post-caffeine APs are boxed in (A).

NIH-PA Author Manuscript

NIH-PA Author Manuscript

NIH-PA Author Manuscript

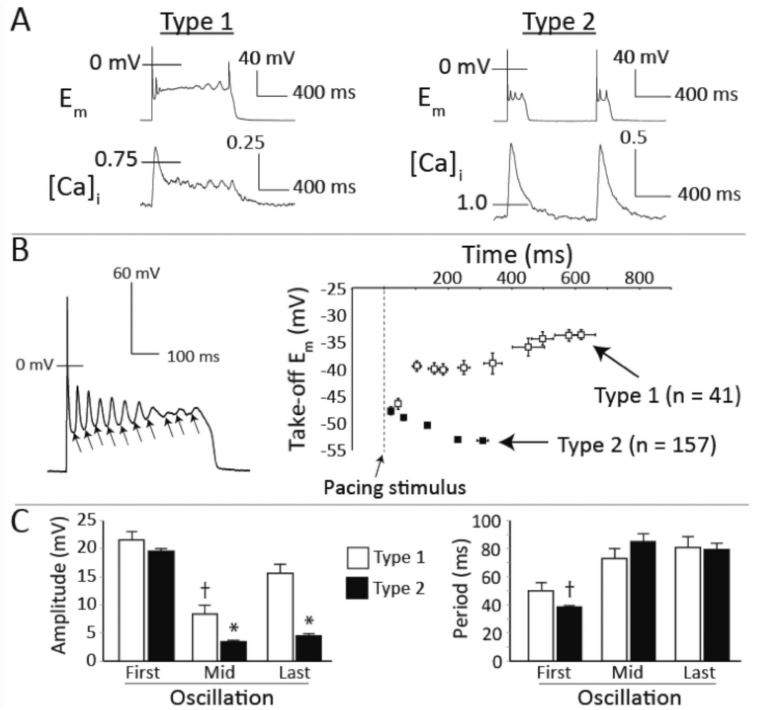

Figure 4.

Multiple mechanisms contribute to murine EADs. A. Representative examples of type 1 (left) and type 2 (right) EADs. B. Left: Representative trajectory for TO potentials within a single AP. Right: Mean trajectories for TO potentials in type 1 and type 2 EAD cycles. C. Average oscillation amplitudes (left) and periods (right) for the initial (First), middle (Mid), and final (Last) oscillations in all type 1 (n=33) and type 2 EAD (n=48) cycles with more than 3 oscillations. * $p < 0.05$ vs. Type 1 (same oscillation) and Type 2 (First oscillation); † $p < 0.05$ vs. Type 1 (First oscillation). Data are mean±SEM.

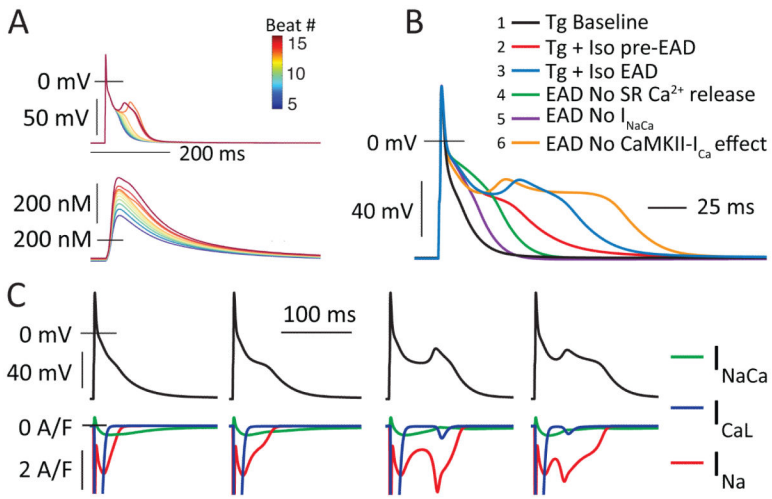

Figure 5.

I_{Na} drives EAD initiation in murine ventricular myocytes. A. A sequence of simulated beats in Iso showing transition through AP prolongation to EAD initiation as whole-cell Ca^{2+} load and SR Ca^{2+} release increases. B. Simulations of the first EAD+ beat in the model where specific components were deleted (only in this beat) to test their acute effects in EAD initiation. The deleted components were: (4) SR Ca^{2+} release ($G_{rel} = 0$); (5) I_{NaCa} ($V_{NCX} = 0$); (6) CaMKII effects at I_{CaL} ($G^{CaL} = 0.3458$, $K_{pc,max}=0.1162$). C. Four APs and corresponding inward currents, showing the role of I_{Na} in both AP prolongation and EAD initiation.

NIH-PA Author Manuscript NIH-PA Author Manuscript NIH-PA Author Manuscript

NIH-PA Author Manuscript

NIH-PA Author Manuscript

NIH-PA Author Manuscript

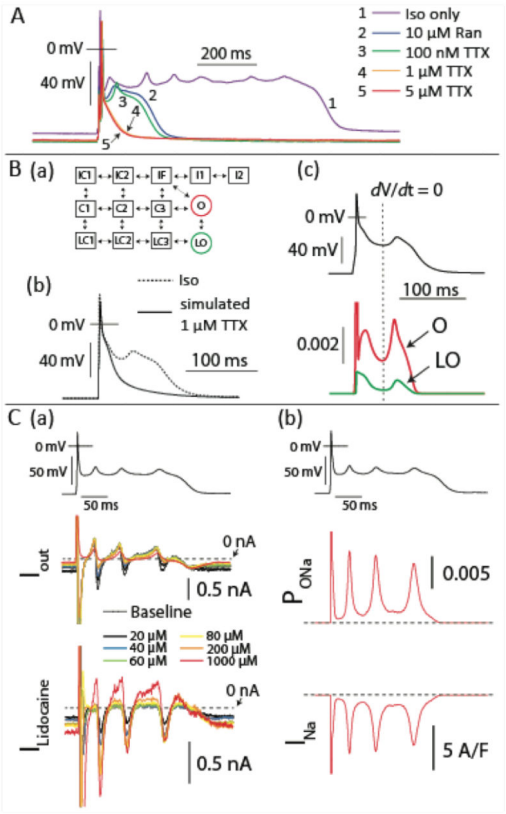

Figure 6.

Non-equilibrium reactivation of I_{Na} carries the EAD upstroke. A. EADs were interrupted first by rapid application of 10 *μM* Ranolazine. After washout, TTX was progressively introduced to the bath and eliminated EADs at 1 *μM*. B. (a) The states of the I_{Na} model: C1-C3 are closed states, LC1-LC3 are burst-mode closed states, IF is the fast inactivation state, I1 and I2 represent intermediate and deeply inactivated channels, and finally, O and LO are the normal and burst-mode open states, respectively. (b) EADs were eliminated by simulated 1 *μM* TTX (50% reduction in G_{Na}). (c) The time course of LO and O occupancies during a simulated EAD, where the canonical open state (O) repopulates before the late open state LO and supports a role for non-equilibrium reactivation of I_{Na} in EAD initiation. C. (a) lidocaine blockade during AP clamp of a WT mouse myocyte indicates that a substantial lidocaine-sensitive current is recruited by the EAD upstroke. At top is the clamped AP waveform (collected in a Tg cell), in the middle is the corresponding raw current (I_{out}), and at bottom is the lidocaine-sensitive difference current ($I_{lidocaine}$). Lidocaine concentrations are shown inset. (c) The same experimental AP waveform is applied to the WT I_{Na} model, and yields similar current reactivation.

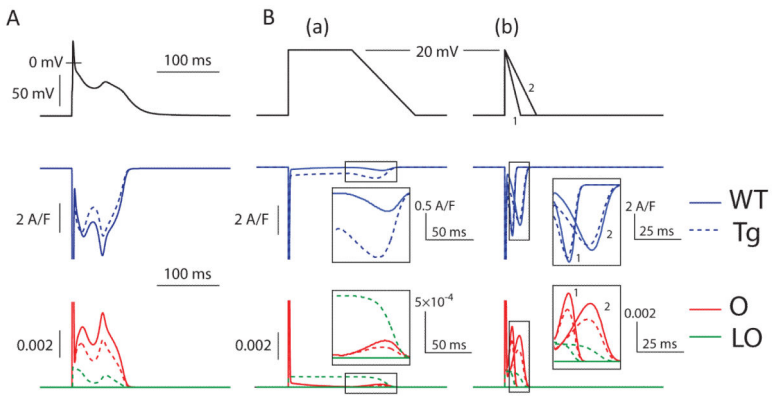

Figure 7.

Simulated CaMKII hyperphosphorylation inhibits rather than promotes non-equilibrium reactivation of I_{Na}. A. Simulated AP clamp of the WT and Tg I_{Na} models[20], using the first AP with an EAD from the Tg+Iso cell model and showing exaggerated reactivation in the WT model. B. Voltage clamp ramp simulations of the WT and Tg I_{Na} models. (a) The slow repolarizing ramp (similar to that used by Clancy et al.) to simulate human repolarization, permits little non-equilibrium reactivation from either I_{Na} model. (b) More rapid repolarizations (1 = 4V/s, 2 = 2V/s) without a preceding plateau permits much greater reactivation, although this is blunted in the Tg I_{Na} model.

NIH-PA Author Manuscript NIH-PA Author Manuscript NIH-PA Author Manuscript